

X-RAY OBSERVATIONS OF THE MASS AND ENTROPY DISTRIBUTIONS IN NEARBY GALAXY CLUSTERS

G.W. PRATT

MPE Garching, Giessenbachstraße, 85748 Garching, Germany

I review some important aspects of the structural and statistical properties of the nearby X-ray galaxy cluster population, discussing the new constraints on mass profiles, the mass-temperature relation, and the entropy of the intracluster medium which have become available from recent X-ray observations.

1 Introduction

Massive systems of galaxies, gas and dark matter, located at the intersection of tenuous, large-scale filaments, galaxy clusters are the nodes of the highly structured Universe we see today. Formed from the collapse of initial density fluctuations, clusters are built hierarchically and constitute an evolving population. The evolution of structure in the Universe – and thus that of clusters – is strongly dependent on the cosmology, so that the statistical properties of the cluster population are a test both of cosmology and of structure formation theory itself.

While clusters were initially discovered as overdensities of galaxies on optical plates, our present understanding of their composition suggests that the galaxies themselves constitute only ~ 5 per cent of the total mass, with most of the mass (~ 80 per cent) in the dark matter component. The dominant baryonic component is the hot, X-ray emitting intracluster medium (ICM), a rarefied plasma at several million K, reflecting the great depth of the potential well in which it lies. We are currently in the privileged position of having several world-class X-ray observatories with which to examine the structural and scaling properties of the ICM in galaxy clusters. The arcsecond spatial resolution of *Chandra* is complemented by the grasp of *XMM-Newton*, allowing spatially-resolved observations to be performed with unprecedented precision^a.

In this paper I begin with a brief review of the expectations for structure and scaling from the starting point of simple gravitational structure formation. I then compare these simple expectations with recent observations of nearby clusters from *XMM-Newton* and *Chandra*. I first show how X-ray observations can be used to place strong constraints on the dark matter component, and then, passing via the $M-T$ relation, I take a look at how measurements of the entropy have cast light on the effect of non-gravitational processes, such as galaxy formation and cooling, on the X-ray properties of the cluster population.

^aIn addition, the recently-launched *Suzaku* X-ray satellite has a much lower instrumental background, holding the promise of spatially resolved observations to larger cluster-centric distances.

2 Expectations for structure and scaling

It is useful to have a baseline prediction for the X-ray properties of the cluster population. Cluster formation is driven by the gravitational collapse of the dominant dark matter component. The ICM collapses with the dark matter, so that, to a first approximation, the gas properties should be determined entirely by the processes involved in gravitational collapse, i.e., shock heating and compression. The baseline model rests on several simple assumptions (e.g., Eke et al., 1998):

- The internal structures of clusters of different mass are similar.
- All clusters identified at a given redshift correspond to a given characteristic density, and the characteristic density scales with the critical density of the Universe, i.e.,

$$\frac{GM_{200}}{R_{200}^3} = \langle \rho \rangle = \frac{4\pi}{3} \delta \rho_c(z); \delta \sim 200. \quad (1)$$

- The ICM evolves in the gravitational potential of the dark matter; the gas mass fraction is thus constant,

$$f_{\text{gas}} = \frac{M_{\text{gas}}}{M_{200}}. \quad (2)$$

- Time-averaged, the ICM is in approximate hydrostatic equilibrium, allowing application of the Virial Theorem, giving:

$$\frac{G\mu m_p M_{200}}{2R_{200}} = \beta_T kT \quad (3)$$

where T is the mean cluster X-ray temperature and β_T is a normalisation constant dependent on internal structure.

The above equations imply that power-law relations exist between various X-ray properties, Q , and the mass M (or a mass proxy) and the redshift, z , such that $Q \propto A(z)M^\alpha$. The evolution factor, $A(z)$, is due to the evolution of the mean density, which varies with the critical density, $\rho_c(z) \propto h^2(z)$. For example, the gas and total mass scale as $M_{\text{gas}} \propto M_{200} \propto h^{-1}(z)T^{3/2}$, and, assuming bremsstrahlung emission, the X-ray luminosity scales as $L_X \propto h(z)T^2$. The assumption of structural similarity further implies that, once scaled appropriately, the radial profiles of various cluster quantities (e.g., gas density ρ , entropy S , temperature T , total mass M) are similar.

Clusters created in hydrodynamical simulations of purely gravitational structure formation are structurally similar and follow these scaling relations (e.g., Bryan & Norman, 1998), showing that the assumptions underlying this simple spherical baseline model are applicable in a hierarchical cosmological context^b. In comparison with observations, the study of both the correlations between global properties (the scaling relations) and the structural properties (radially-averaged profiles of various quantities) is essential for the best understanding of cluster formation and evolution.

^bNote that there is a certain amount of intrinsic scatter in the relations, which is related to cluster dynamics.

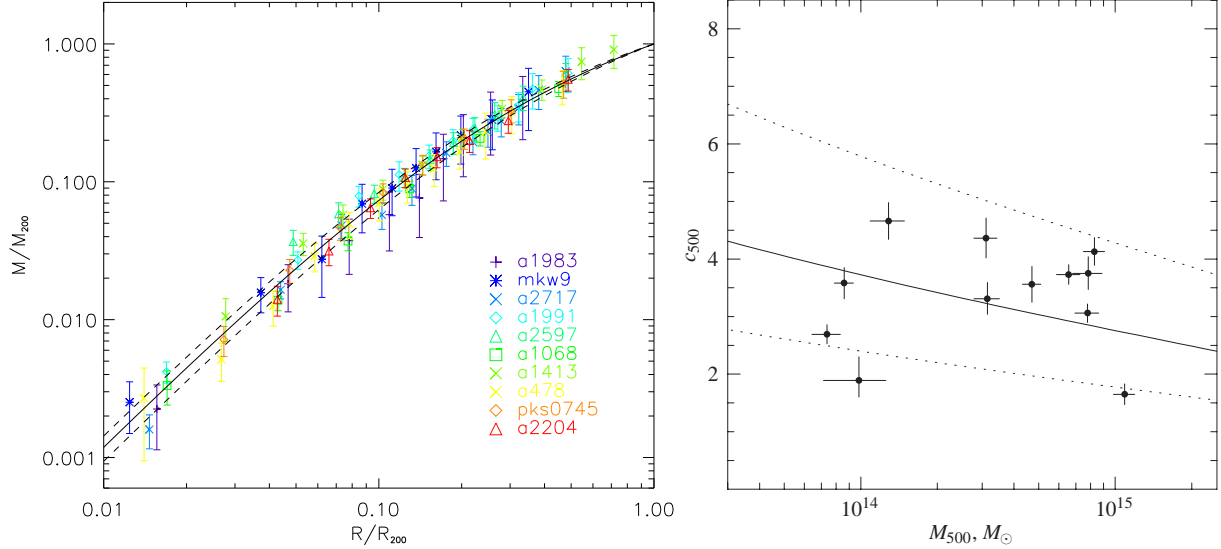


Figure 1: **Left:** Integrated mass profiles of 10 clusters in the temperature range 2 - 9 keV, observed with *XMM-Newton* (from Pointecouteau et al., 2005). For each cluster, the mass is scaled to M_{200} and the radius to R_{200} . The black line corresponds to the mean scaled best-fitting NFW model; the dashed lines the associated standard deviation. **Right:** Concentration parameter vs mass relation for NFW model fits to the total density profiles of 12 clusters in the temperature range 0.7 - 9 keV, observed with *Chandra* (from Vikhlinin et al., 2006). The solid line shows the average concentration of CDM haloes from simulations; the dotted lines show the associated 2σ scatter.

3 Dark matter constraints

3.1 Mass profiles

An inescapable prediction from more than a decade's worth of numerical simulations is the existence in haloes of a semi-universal cusped dark matter density profile. The most well-known variant is the Navarro-Frenk-White (Navarro et al., 1997, NFW) profile, $\rho_{DM}(r) \propto [(r/r_s)(1+r/r_s)^2]^{-1}$, where the concentration parameter, $c_\delta = R_\delta/r_s$, is a measure of the halo concentration. The profile is not strictly universal since there is a weak dependence of c_δ on mass, M_δ , due to the fact that smaller mass haloes generally form earlier, when the Universe was denser (Bullock et al., 2001; Dolag et al., 2004). Although the total mass density profile can be measured with both X-ray and optical observations, in the latter case, stacking is often required to overcome the paucity of data on individual objects if quantitative measurements of the mass profile are to be obtained (e.g., Biviano & Girardi, 2003). In contrast, while X-ray observations allow measurements of individual mass density profiles, the method relies on the assumption that the gas is in hydrostatic equilibrium.

X-ray observational confirmation of the existence of a cusped profile on cluster scales started to become available with *ASCA* observations (Markevitch et al., 1999), although the spatial resolution of these observations, in particular of the temperature profiles, was not optimal. More recent observations with *XMM-Newton* and *Chandra* have allowed the mass profiles of relaxed clusters to be probed from the very core regions ($\sim 0.01R_{200}$, e.g., Lewis et al., 2003) right out to $0.7 - 0.8 R_{200}$ (i.e., $\sim R_{500}$; Pratt & Arnaud, 2002; Pointecouteau et al., 2004; Vikhlinin et al., 2006). All of these observations point to the existence of a quasi-universal cusped profile as predicted from CDM simulations. There is no evidence for a core in even the highest-resolution observations (Lewis et al., 2003), effectively ruling out the possibility of self-interacting dark matter on cluster scales.

3.2 Concentration parameters

Observations of small samples of clusters and galaxy groups have also allowed the universality of mass and total density profiles to be probed (Pratt & Arnaud, 2005; Pointecouteau et al., 2005; Vikhlinin et al., 2006; Humphrey et al., 2006). The left-hand panel of Fig. 1 shows the integrated mass profiles of 10 clusters in the temperature range 2 - 9 keV, scaled by the virial mass M_{200} and radius R_{200} . The mass profiles can all be adequately fitted with NFW models and are clearly similar once scaled in this manner. The right-hand panel of Fig. 1 shows the measured concentration parameters from fits to the total density profile of 12 clusters in the temperature range 0.7-9 keV (Vikhlinin et al., 2006), compared to the theoretical predictions of Dolag et al. (2004). The observed concentration parameters are in good agreement, both in absolute value and dispersion, with the theoretical predictions. Similar results have been found by Pointecouteau et al. (2005) for another sample of clusters, and by Humphrey et al. (2006) for a sample of galaxy groups. In the latter case, it was found that inclusion of a stellar mass component was necessary to give acceptable fits to the data, since this component starts to dominate the mass budget in the very inner regions (see also Lokas & Mamon 2005). Such results are encouraging and have allowed constraints to be put on the nature of the dark matter itself on cluster scales, suggesting that our understanding of the dark matter collapse is correct down to the scale of individual giant galaxies.

Finally, it should be pointed out that all of the above results were obtained only for morphologically relaxed systems. Attempts to model the total mass density profiles of less relaxed systems with the NFW profile have resulted in poor fits (Belsole et al., 2005; Pratt et al., 2005). This suggests that in these cases either (i) the gas is not in hydrostatic equilibrium, or (ii) that the underlying DM density profile is not well described by an NFW model (the original NFW model was proposed specifically for systems with a relatively high degree of relaxation).

4 The M - T relation

Models of structure formation predict the space density, distribution and physical properties of the cluster population as a function of mass and redshift, so that, from the theoretical point of view, the mass of a cluster is its most fundamental property. However, X-ray cluster surveys yield the cluster space density and distribution only in terms of X-ray observables such as the luminosity, L_X , or the temperature T . Scaling relations linking the mass to the X-ray observables allow the full use of X-ray cluster survey information in the statistical sense. Knowledge of mass observable relations and the associated scatter about these relations is thus crucial in the use of clusters to probe cosmology.

Assuming hydrostatic equilibrium and spherical symmetry, the mass of a cluster can be recovered from spatially-resolved X-ray observations of the density and temperature profiles. The M - T relation is one of the fundamental relations for linking the observed gas properties with theory, since the temperature is expected to be closely related to the mass via the Virial theorem. It is also of topical interest, since the normalisation of this relation has a direct bearing on the measurement of the present-day value of σ_8 using cluster abundance measurements, and, until the WMAP 3-year data, cluster measurements of σ_8 were thought to be unusually low. Samples from *ROSAT* and *ASCA*, though large, either assumed that clusters were isothermal (Horner et al., 1999; Xu et al., 2001; Castillo-Morales & Schindler, 2003) or had relatively poor temperature profile resolution and/or relied strongly on extrapolation to derive the virial mass (Nevalainen et al., 2000; Finoguenov et al., 2001; Sanderson et al., 2003). As a result, historically, there has been little consensus on either the slope or the normalisation of the M - T relation.

The situation is much improved with recent results from *XMM-Newton* and *Chandra*. The left-hand panel of Figure 2 shows the mass-temperature data from two cluster samples

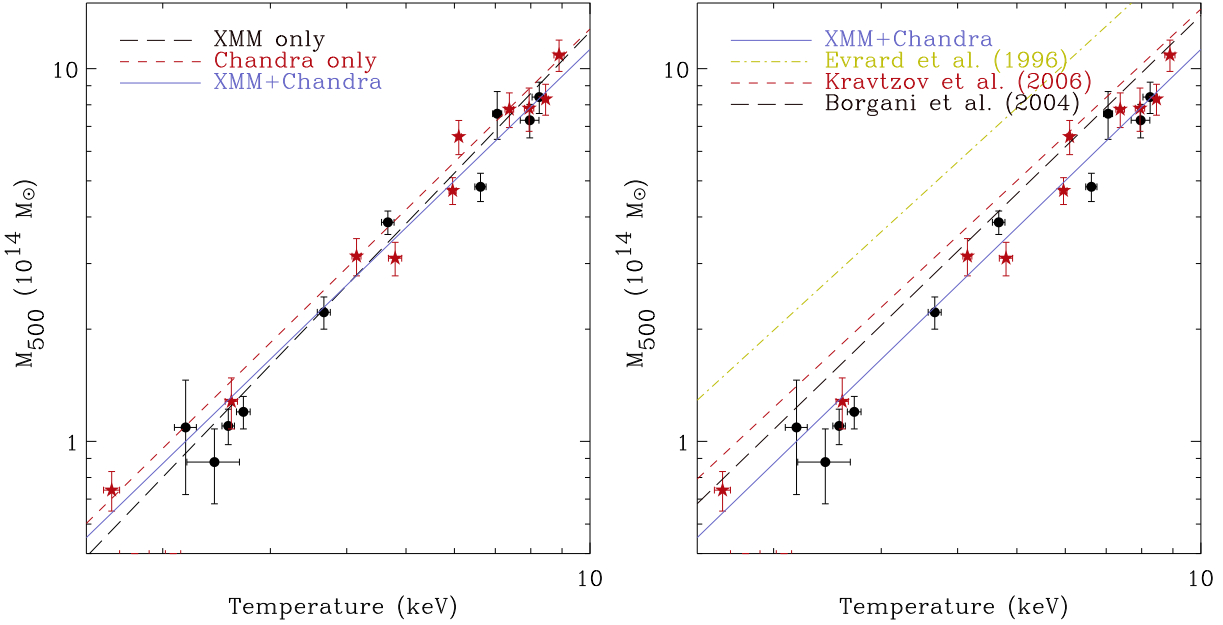


Figure 2: **Left:** The X-ray mass-temperature relation from observations obtained with *XMM-Newton* (Arnaud et al., 2005, circles) and *Chandra* (Vikhlinin et al., 2006, stars). Some clusters were observed with both satellites, and are plotted twice; note that the measurements agree within the 1σ errors. The long-dashed line is the best-fitting relation to the *XMM-Newton* data points, the dashed line is the best fitting relation to the *Chandra* points, and the solid lines is the best fitting relation to all data points. See text for details. **Right:** Comparison with results from several numerical simulations. The inclusion of more realistic physical processes in more recent simulations has improved the agreement between observation and theory.

observed independently with *XMM-Newton* (Arnaud et al., 2005) and *Chandra* (Vikhlinin et al., 2006)^c. The various lines show the results of fitting a power-law function of the form $h(z)M = A \times (kT/5 \text{ keV})^\alpha$ to different data sets. The fits to the individual *XMM-Newton* and *Chandra* data sets give results which are entirely consistent within the 1σ errors for both slope and normalisation. A BCES fit to the total data set yields the relation

$$\log [h(z)M_{500}/10^{14} M_\odot] = (0.57 \pm 0.02) + (1.59 \pm 0.08) \log [kT/5 \text{ keV}]. \quad (4)$$

The slope is thus very close to the expectations from the simple scaling analysis in Sect. 2 above.

A second historical point of contention is the disagreement between the observed M - T normalisation and that derived from numerical simulations. Now that there is good agreement between measures of the observed normalisation, the time is ripe for a new comparison with simulations. The right-hand panel of Figure 2 shows the data and best fitting power law described above, compared to the relations found in the simulations of Evrard et al. (1996), which only include gravitational processes, and the more recent simulations of Borgani et al. (2004) and Kravtsov et al. (2006), which include additional physical processes such as radiative cooling and feedback from supernovae. The disagreement with the gravitation-only simulations is well documented and for the present data set amounts to a difference in normalisation of 40 per cent at 5 keV. The agreement has clearly improved with the introduction of more realistic physical processes into the simulations.

The remaining discrepancy is likely due to a combination of two effects. Firstly, it is unclear how simplifying assumptions of the X-ray analysis have an impact on the final mass determination. In particular, the validity of the assumption of hydrostatic equilibrium has often been

^cSimilar results were found at R_{2500} for a smaller sample of 6 systems by Allen et al. (2001)

called into question. Observations of Coma suggest a lower limit of ~ 10 per cent of the total ICM pressure in turbulent form (Schuecker et al., 2004). However, Coma is a merging cluster and at present no observational constraints exist for the amount of non-thermal pressure support in clusters which observers would call ‘relaxed’. Secondly, the value of the $M-T$ normalisation can vary by up to 50 per cent depending on the simulation (Arnaud et al., 2005; Henry, 2004), and the normalisation has been creeping downwards over time as more complex physics has been incorporated into the simulations. Current simulations are still unable to reproduce not only the observed scaling relations (e.g., the L_X-T relation), but also the structural properties of clusters (e.g., temperature profiles in the central regions), clearly pointing to the possibility that certain physical processes may be missing. Below I discuss how X-ray observations can give an idea of what other physical processes may be in play.

Finally, it should be noted that the above results were obtained for morphologically relaxed cluster samples only. Since the precision on the estimation of cosmological parameter estimation depends on the precision to which the scaling relations are known (e.g., Henry, 2004), accurate estimates of the dispersion around the best fitting relations are needed *for the whole cluster population*. This is true even for the case of self-calibration of extremely large samples. The challenge now is to derive accurate mass-observable scaling relations for *representative* cluster samples. Since the X-ray method is clearly invalid for clusters which are not in hydrostatic equilibrium, this will require inter-calibration of the available mass estimators (X-ray, optical, lensing), preferably using both observed and simulated data sets.

5 Gas physics

X-ray data have been telling us for nearly two decades that the simple scaling relations outlined in Sect. 2 do not describe the observed cluster population. The most well-studied example is that of the L_X-T relation, which has been found by many studies to be $L_X \propto T^3$ (Edge & Stewart, 1991; Arnaud & Evrard, 1999; Markevitch, 1998; Osmond & Ponman, 2004), corresponding to a suppression of X-ray luminosity in poor systems relative to simple expectations. This suggests that physical processes other than gravity alone are affecting the properties of the ICM, and that poorer (i.e., lower temperature) systems are proportionally more affected. These non-gravitational processes are likely linked to radiative cooling and to heating processes associated with galaxy formation.

The entropy affords the most direct way of investigating the properties of the ICM gas. The entropy^d is generated in shocks as the gas falls into the deep potential of the cluster halo. Entropy is conserved in any adiabatic rearrangement of the gas, and the gas will always rearrange itself so that the entropy increases outwards. This property is illustrated in the left-hand panel of Fig. 3, which shows the entropy profiles of 40 clusters spanning a mass range of a factor of ten, from simulations including only gravitational processes (Voit et al., 2005). The profiles have been scaled by the characteristic entropy of the halo

$$K_{200} = \frac{1}{2} \left[\frac{2\pi G^2 M_{200}}{15 f_b H(z)} \right]^{2/3}, \quad (5)$$

where f_b is the baryon fraction, and the radii have been scaled to the virial radius R_{200} . It can be seen that the profiles all coincide, and that, outside the central regions (where gravitational softening becomes important in the simulations), a power-law model with $K \propto R^{1.1}$ is an adequate description of the trend with radius. In the right-hand panel of Fig. 3, I show the entropy profiles of ten morphologically relaxed clusters spanning the temperature range 2–10

^dHere I follow the established convention and refer to the quantity $S = K = kTn_e^{-2/3}$ as the entropy. This is related to the true thermodynamic entropy via $s = \ln K^{3/2} + \text{constant}$.

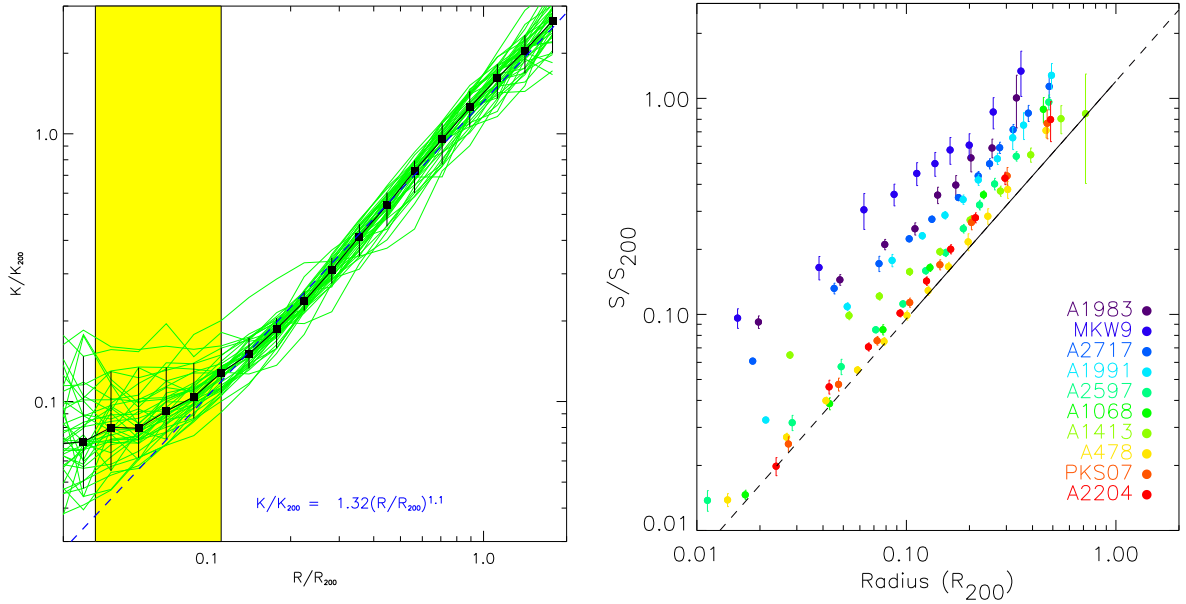


Figure 3: **Left:** Entropy profiles of 40 clusters spanning the mass range $0.2 - 8 \times 10^{14} h^{-1} M_{\odot}$ from simulations including only gravitational processes (from Voit et al., 2005). The profiles have been scaled using the characteristic entropy of the halo K_{200} and the virial radius R_{200} (see text for details). **Right:** Entropy profiles of 10 clusters spanning the mass range $1 - 12 \times 10^{14} h_{70}^{-1} M_{\odot}$ (~ 2 [blue] - 8 keV [red]), observed with *XMM-Newton* (from Pratt et al., 2006). The profiles have been scaled in exactly the same manner. The solid line is the best-fitting power law description of the radial dependence of the entropy for the simulated clusters.

keV ($\sim 10^{14} - 10^{15} M_{\odot}$), observed with *XMM-Newton* (Pratt et al., 2006). The clusters are colour-coded so that poor (cool, low mass) clusters are blue and rich (hot, high mass) clusters are red. They have been scaled in exactly the same manner as the simulated profiles, assuming $f_b = 0.14$ ($\Omega_b h^2 = 0.02$ and $\Omega_m = 0.3$), and the solid line denotes the best-fitting power-law entropy-radius relation to the scaled simulated clusters. It can be seen that, while the profiles of rich clusters are in good agreement (both in slope and in normalisation) with the prediction from gravitational entropy generation, poor clusters have a systematically higher entropy throughout the ICM.

We can get an idea of the dependence of the offset with temperature (or mass) by looking at the entropy measured at a certain fraction of the virial radius. The entropy-temperature $S-T$ (or $K-T$) relation was extensively investigated using data from the previous generation of X-ray satellites. In the simple baseline model outlined in Sect. 2, the gas mass fraction is constant, implying a constant gas density and thus a simple linear scaling of the entropy with temperature $S \propto h(z)^{-4/3}T$, or mass $S \propto h(z)^{-2/3}M^{2/3}$. Initial measurements of the entropy at $0.1 R_{200}$ (Ponman et al., 1999) showed a levelling-off of the $S-T$ relation towards lower temperatures, which was subsequently interpreted as a limiting value to the central entropy (Lloyd-Davies et al., 2000). However, deeper investigation with larger samples observed with *ROSAT* and *ASCA* (Ponman et al., 2003), and smaller samples observed with the newest generation of satellites (Pratt et al., 2006) have shown that there is in fact a continuous power-law relationship between the entropy at a fixed fraction of the virial radius and the temperature, such that $S \propto T^{0.65}$ (see the left-hand panel of Fig. 4). This slope is in agreement with that expected from the observed scaling of X-ray luminosity with temperature. The equivalent entropy-mass relation is $S \propto M^{0.36}$, again shallower than expectations from simple gravitational collapse (Pratt et al., 2006).

High resolution entropy profiles can give essential insights into the physical processes at

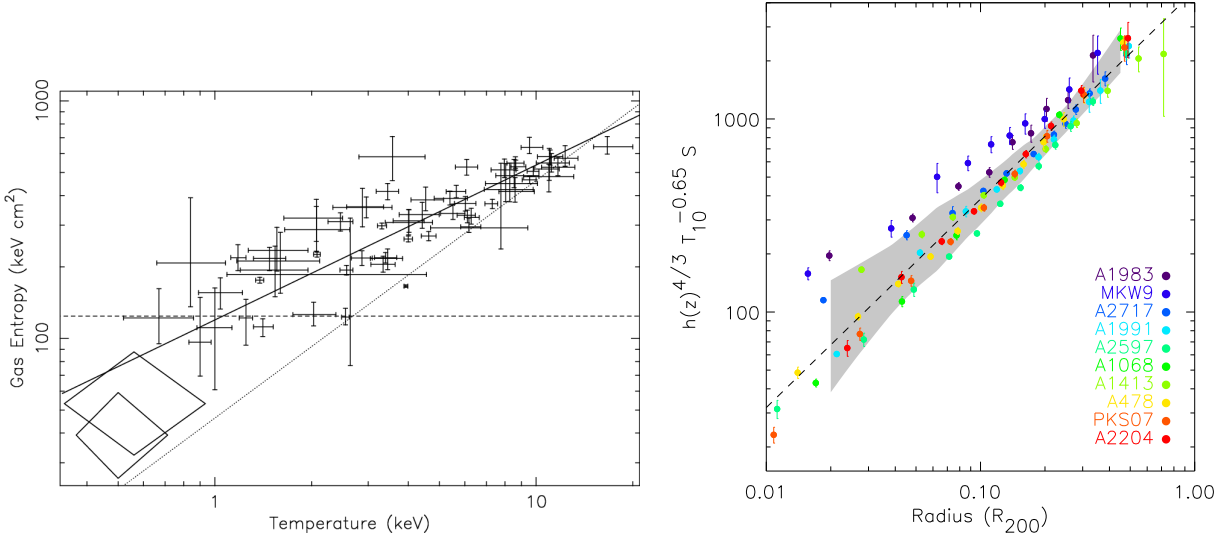


Figure 4: **Left:** Entropy measured at $0.1 R_{200}$ vs system temperature for 66 systems (from Ponman et al., 2003). The dotted line shows the relation expected from pure gravitational structure formation ($S \propto T$). The solid line is the best-fitting power law relation: $S \propto T^{0.65}$. **Right:** Entropy profiles of 10 clusters spanning the mass range $1 - 12 \times 10^{14} h_{70}^{-1} M_\odot$ (~ 2 [blue] - 8 keV [red]), observed with *XMM-Newton* (from Pratt et al., 2006). The profiles have been scaled using the best-fitting empirical entropy scaling.

play. The right-hand panel of Fig. 4 shows the entropy profiles of the same ten clusters from Fig 3, this time rescaled by the observed empirically-determined entropy-temperature relation ($S \propto T^{0.65}$; see also Piffaretti et al., 2005). Two important points are evident from this exercise. Firstly, outside the core regions, the entropy profiles show a remarkable degree of similarity, and the radial dependence of entropy is well described by the relation $S \propto R^{1.1}$, as expected from standard gravitational collapse (Sect. 2), and as is seen in gravitation-only simulations (Voit et al., 2005). Thus non-gravitational processes appear to alter the power-law scaling of the entropy-temperature relation without breaking structural similarity, at least for clusters of this mass range and above (results for the group regime $\lesssim 2$ keV are less conclusive, see Mahdavi et al. 2005). It is still unclear what mechanism is causing this effect. One proposal is that smoothing of the gas density due to preheating in filaments and/or infalling groups may boost entropy production at the accretion shock (Voit et al., 2003; Ponman et al., 2003). However, numerical simulations run specifically to test this effect seem to suggest that the boosting, though present, appears to be substantially diminished in the presence of radiative cooling (Borgani et al., 2005). The same simulations suggest that feedback from supernovae is too localised to have a significant effect on smoothing of the accreting gas. Another possibility is that activity from the central AGN produces the extra heating, although the observed normalisations require that the AGN affects the entropy distribution in a non-catastrophic manner at least out to R_{1000} ($\sim 0.5 R_{200}$) and it is not clear why and how this would produce the observed power-law entropy-temperature dependence.

Secondly, inside the core regions the dispersion increases dramatically, constituting an effective breaking of similarity. Three probable mechanisms for breaking of similarity in the core are radiative cooling, AGN feedback, and mixing of high and low entropy gas due to merging activity. Disentangling the effects of these processes will require a concerted effort from both observations and simulations.

6 Summary and perspectives

The explosion of high quality data available from the most recent generation of X-ray satellites has allowed unprecedented insights to be gained into cluster physics. The parallel increase in computing power available for large hydrodynamic simulations has facilitated increasingly sophisticated comparisons between observations and theory. The resulting cross-fertilisation has had profoundly beneficial effects on our understanding of the formation and evolution of structure in the Universe.

X-ray observations have allowed strong constraints to be put on the form of the mass density profile in clusters, suggesting a cusped form and a variation with mass in agreement with the predictions from numerical simulations. This result is true over the entire measurable radial range ($\sim 0.001\text{--}0.8 R_{200}$) in morphologically relaxed clusters, groups, and individual galaxies.

The observed X-ray mass-temperature ($M\text{--}T$) relation has been measured using data from *XMM-Newton* and *Chandra* with several samples of moderate size, yielding results which are in very good agreement both in terms of slope and normalisation. This agreement can be attributed both to better data quality and to improved data analysis techniques. However, there is still an offset between the observed $M\text{--}T$ normalisation and that determined from numerical simulations. While a part of this discrepancy may come from details of the X-ray analysis (perhaps principally the assumption of hydrostatic equilibrium), it is also clear that since simulations currently do not reproduce the gross scaling properties of the cluster population (e.g., the $L_X\text{--}T$ relation) the physics governing the baryonic component are incompletely understood.

We can get an insight into this by looking at the entropy of the ICM. The entropy-temperature relation is shallower than expected, $S \propto T^{0.65}$, such that poor systems have higher entropy than rich systems relative to that expected from pure gravitational collapse. Entropy profiles of clusters formed purely through gravitational processes are self-similar (once scaled appropriately) and are characterised by a radial dependence $S \propto R^{1.1}$ outside the central regions ($R > 0.1 R_{200}$), a slope characteristic of shock heating of the ICM. The entropy profiles of observed clusters are self-similar outside the central regions once scaled by the empirical scaling, and display a slope similar to that expected from shock heating. Thus the entropy is higher throughout the ICM in poor systems. It is not yet clear what physical mechanism is responsible, but the most obvious candidates are preheating and AGN activity. In the central regions ($R < 0.1 R_{200}$), there is a clear breaking of similarity. This is probably due to the combined action of radiative cooling, AGN heating and mixing of high and low entropy gas during mergers.

Most of the above results have been derived from observations of morphologically relaxed systems, and are thus they are neither representative of the cluster population as a whole, nor useful from the point of view of establishing the intrinsic scatter about the scaling relations. The challenge now is in the observation of larger samples with unbiased mass and redshift sampling. These should be used to i) further test the self-similarity of form; ii) derive the exact slope, normalisation and intrinsic scatter of the $M\text{--}T$ relation, requiring cross-calibration and combination of different mass estimation methods including X-ray, lensing, and dynamical; iii) compare with state of the art simulations to probe the sources and timescales of the non-gravitational energy input which alters the similarity of the cluster population.

Acknowledgements

I would like to thank Sophie Maurogordato and Laurence Tresse for organising such an excellent meeting, and the Program and Scientific Advisory Committees for the invitation to present this review and for partial financial support. I warmly thank my collaborators for their contributions to some of the papers discussed in this review. This work received partial support from a Marie Curie Intra-European Fellowship (Contract No. MEIF-CT-2003-500915).

References

Allen, S.W., Schmidt, R.W., Fabian, A.C., 2001, MNRAS, 328, L37

Arnaud, M., Evrard, A.E., 1999, MNRAS, 305, 631

Arnaud, M., Pointecouteau, E., Pratt, G.W., 2005, A&A, 441, 893

Belsole, E., Sauvageot, J.L., Pratt, G.W., Bourdin, H., 2005, A&A, 430, 385

Biviano, A., Girardi, M., 2003, ApJ, 585, 205

Borgani, S., Murante, G., Springel, V., et al., 2004, MNRAS, 348, 1078

Borgani, S., Finoguenov, A., Kay, S.T., et al., 2005, MNRAS, 361, 233

Bryan, G.L., Norman, M.L., 1998, ApJ, 495, 80

Bullock, J.S., et al., 2001, MNRAS, 321, 559

Castillo-Morales, A., Schindler, S., 2003, A&A, 403, 433

Dolag, K., Bartelmann, M., Perrotta, F., et al., 2004, A&A, 416, 853

Edge, A.C., Stewart, G.C., 1991, MNRAS, 252, 414

Eke, V.R., Navarro, J.F., Frenk, C.S., 1998, ApJ, 503, 569

Evrard, A.E., Metzler, C.A., Navarro, J.F., 1996, ApJ, 469, 494

Finoguenov, A., Reiprich, T.H., Böhringer, H., 2001, A&A, 368, 749

Henry, J.P., 2004, ApJ, 609, 603

Horner, D.J., Mushotzky, R.F., Scharf, C.A., 1999, ApJ, 520, 78

Humphrey, P.J., Buote, D.A., Gastaldello, F., et al., 2006, ApJ, in press (astro-ph/0602613)

Kravtsov, A.V., Vikhlinin, A., Nagai, D., 2006, A&A, submitted (astro-ph/0603205)

Lewis, A.D., Buote, D.A., Stocke, J.T., 2003, ApJ, 586, L135

Lloyd-Davies E.J., Ponman, T.J., Cannon, D.B., 2000, MNRAS, 315, 689

Lokas, E.L., Mamon, G.A., 2005, MNRAS, 362, 95

Mahdavi, A., Finoguenov, A., Böhringer, H., et al., 2005, ApJ, 622, 187

Markevitch, M., 1998, ApJ, 504, 27

Markevitch, M., Vikhlinin, A., Forman, W.R., Sarazin, C.L., 1999, ApJ, 527, 545

Navarro, J.F., Frenk, C.S., White, S.D.M., 1997, ApJ, 490, 493

Nevalainen, J., Markevitch, M., Forman, W.R., 2000, ApJ, 536, 73

Osmond, J.P., Ponman, T.J., 2004, MNRAS, 350, 1511

Piffaretti, R., Kaastra, J.S., Jetzer, Ph., Tamura, T., 2005, A&A, 433, 101

Pointecouteau, E., Arnaud, M., Kaastra, J., de Plaa, J., 2004, A&A, 423, 33

Pointecouteau, E., Arnaud, M., Pratt, G.W., 2005, *A&A*, 435, 1

Ponman, T.J., Cannon, D.B., Navarro, J.F., 1999, *Nature*, 397, 135

Ponman, T.J., Sanderson, A.J.R., Finoguenov, A., 2003, *MNRAS*, 343, 331

Pratt, G.W., Arnaud, M., 2002, *A&A*, 394, 375

Pratt, G.W., Arnaud, M., 2005, *A&A*, 429, 719

Pratt, G.W., Böhringer, H., Finoguenov, A., 2005, *A&A*, 433, 777

Pratt, G.W., Arnaud, M., Pointecouteau, E., 2006, *A&A*, 446, 429

Sanderson, A.J.R., Ponman, T.J., Finoguenov, A., et al., 2003, *MNRAS*, 340, 989

Schuecker, P., Finoguenov, A., Böhringer, H., et al., 2004, *A&A*, 426, 387

Vikhlinin, A., Kravtsov, A., Forman, W.R., et al., 2006, *ApJ*, 640, 691

Voit, G.M., Balogh, M.L., Bower, R.G., et al., 2003, *ApJ*, 593, 272

Voit, G.M., Kay, S.T., Bryan, G.L., 2005, *MNRAS*, 364, 909

Xu, H., Jin, G., Wu, X.P., 2001, *ApJ*, 553, 78